Equivalent Dipole Trajectories Assessed From the 12-Lead ECG Using a Tailored Human Torso Model

Vito Starc[1]

[1]University of Ljubljana, Faculty of Medicine, Ljubljana, Slovenia

Abstract

We extended our application for the assessment of moving equivalent dipoles (ED) from the surface ECG by incorporating a BEM method to calculate potentials on the surface of a tailored human torso model and explored whether it could provide reliable ED trajectories from the 12-lead ECGs compared to those from the body surface potential map (BSPM) data.

We used 17 recordings of the Dalhousie BSPM data (EDGAR) with ECG signals arising from different pacing sites in the same patient and tested for the congruency of the derived ED trajectory patterns of the 12-lead and BSPM data sets. We found that the ED trajectories from these two sets are mutually shifted or rotated by less than the median offset of 1.5 cm and deviation angle of 15º.

We believe that assessing the ED trajectory with this accuracy may help improve the detection of depolarization abnormalities in the clinical setting.

1. Introduction

Recently, it has been shown by different analytical approaches that it is possible to detect changes in the location of the current source in the heart connected with different cardiac pathologies from 12-lead ECG. These approaches included the assessment of moving equivalent dipoles (ED) and its trajectory [1,2] or the derivation of the mean temporal-spatial isochrones [3]. Common in all approaches were uncertainties in determining the exact position of the ED trajectory in space. It was usually bypassed by assuming that during depolarization, the trajectory center coincides with the ventricular center.

We explored whether our upgraded application could provide reliable ED trajectories from the 12-lead ECGs by evaluating them by comparing them to the ED trajectories derived from the body surface potential map (BSPM) data set. We extended our application by incorporating a BEM method to calculate potentials on the surface of a tailored human torso model, which enables the determination of equivalent dipoles (ED) from the measured body potentials (the inverse model). In addition to the standard 12-lead ECG set (LeadSet1), we used a modified 12-lead ECG set (LeadSet2) by displacing three precordial leads to increase the space isotropy in the lead positions. Besides, we tested an assumption that EDs move along the direction of the ED orientation during depolarization of the heart.

2. Methods

1.2. Construction of a tailored torso model

A patient-specific torso was introduced by tailoring the torso considering individual anthropometric measures, such as the torso height, width and depth at the level of the shoulders, waist and the hip. The torso framework consists of 24 vertically aligned rounded isosceles trapezoids with legs at an angle or below 12º and with circles inscribed at the trapezoid corners. The trapezoid shape is tailored from the neck to the hip to fit individual anthropometric data (Figure 1). Each trapezoid is divided into 48 sectors using successive lines from the trapezoid center to its border with the azimuth angle increasing by 7.5º. The border intersection points serve as surface nodes for determination of N=1152 quadrangular torso surfaces when connecting four neighboring nodes of two adjacent trapezoids.

2.2. Calculation of surface potentials

The central points of the discretized surfaces at positions $\mathbf{r}_i$, i=1 to N, were utilized for the determination of surface potentials φ_i using the boundary element model (BEM) that relates the distribution $\boldsymbol{\varphi}$ to the inverted matrix $\mathbf{A}^{-1}$, $\boldsymbol{\varphi} = \mathbf{A}^{-1}\,\mathbf{g}$ [4]. The matrix $\mathbf{A}^{-1}$ is obtained by inverting a deflated matrix $\mathbf{A} = \mathbf{B} - \mathbf{I}$, where $\mathbf{B}$ depends on all mutual solid angles among discretization points and local volume conductivities, and $\mathbf{I}$ is a unitary matrix. The vector $\mathbf{g}$ represents the potentials $\varphi_{\infty,i}$ at $\mathbf{r}_i$ generating by dipole vector $\mathbf{D}_k$ (the current source) at the position $\mathbf{r}_k$ in an infinite medium, $\varphi_{\infty,i} = \boldsymbol{\rho}_{ki} \cdot \mathbf{D}_k$, where $\rho_{ki} =$

$(1/4\pi\sigma)\,\Delta \boldsymbol{r}_{ik}/|\Delta \boldsymbol{r}_{ik}|^3$ and $\Delta\mathbf{r}_{ki} = \mathbf{r}_i - \mathbf{r}_k$ are vectors. The inverse $\mathbf{A}^{-1}$ is obtained by LU decomposition of matrix **A**, and the potentials at the discretization points with LU back substitution.

If the skalar component g_i of vector **g** is written as a dot product of its spatial and dipolar components, $\boldsymbol{\rho}_{ik}$ and $\mathbf{D}_k$, respectively, the forward model provides

$$\varphi_{ik} = \mathbf{L}_{ik} \cdot \mathbf{D}_k, \qquad (1)$$

where $\mathbf{L}_{ik} = \mathbf{A}^{-1}\boldsymbol{\rho}_{ik}$ represents the Burger's lead vector. This formulation provides a linear dependence of φ_{ik} on cartesian $\mathbf{D}_k$ components, $\varphi_{ik}=L_{ikx}\cdot D_{kx}+L_{iky}\cdot D_{ky}+ L_{iky}\cdot D_{ky}$, that facilitates calculation but requires a separate determination of $\mathbf{L}_{ik}$ components in x, y and z directions. In the case of a reduced set of N_l electrodes providing N_l signals, the dimension of $\boldsymbol{\varphi}$ is reduced to N_l, if electrodes coincide with the outer surface's discretization points. Otherwise, additional potentials are required for the interpolation.

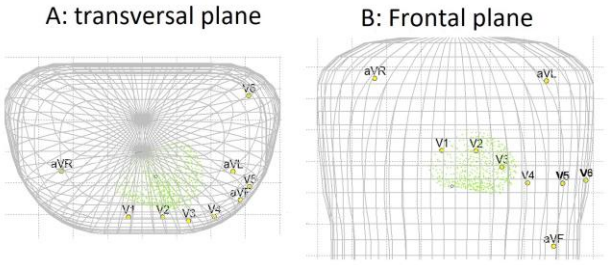

Figure 1. Human torso model with the standard 12-lead electrode positions with discretized quadrangular surfaces on B.

2.3. The assessment of the ED trajectory

To find a set of moving equivalent dipoles $\mathbf{D}_k$ with locations $\mathbf{r}_k$ (dipolar trajectory) that best describe measured signals $\mathbf{V}_{ik}$, denoting signal samples with index k, we applied an optimization method with the objective function $\psi(\mathbf{r}_k)$ that minimizes the error $\mathbf{F}_{ik}=|\boldsymbol{\varphi}_{ik}-\mathbf{V}_{ik}|$ between the model predicted and measured potentials represented by N_l signals with N_k samples,

$$\psi(\boldsymbol{r_k}) = \sum_k^{N_k}\left(\sum_i^{N_l}\|\boldsymbol{F_{ik}}\|^2 + \|R\|\right), \qquad (2)$$

where R represents some positive valued regularizing function [5], such as the trajectory curvature, deviation from the measured electrode position, local conductivities or deviation from the Wilson central terminal.

During optimization, the set of $\mathbf{r}_k$ was varied and at each iteration, the $\mathbf{D}_k$ set was determined the following way. In a lead set with N_i electrodes (N_{ECG}=9 for standard ECG and N_{BSPM}=120 for BSPM) and with a given set of $\mathbf{r}_k$ (the trajectory), the set of signals forms an overdetermined system of Ni equation with 3 unknowns D_{kx}, D_{ky} and D_{kz} that are linearly related to the measured $\mathbf{V}_{ik}$. To solve it, we applied principal component analysis to find $\mathbf{D}_k$ that minimizes the sum of the squared errors $\mathbf{F}_{ik}$ separately for each $\mathbf{r}_k$. Each successive iteration provided smaller $\mathbf{F}_{ik}$ and better $\mathbf{D}_k$ until reaching the minimal $\psi(\mathbf{r}_k)$ and the optimal set of $\mathbf{r}_k$. The square root of $\psi(\mathbf{r}_k)$ normalized with the sum of the squared potentials $\mathbf{V}_{ik}$ represented the root normalized mean square error (RNMSE).

2.4. Description and analysis of ECG data

We used 17 recordings of the Dalhousie BSPM data (EDGAR) representing ECG signals arising from different pacing sites (e.g., pacing from the apical septum, infero-posterior apex, LVOT, or with RBBB and LBBB morphology) in the same patient (Figure 2) [6,7]. All signals with resolution 1kHz containing the complete QT interval were corrected for the Wilson central terminal, WCT= (I+II)/3.

To test the hypothesis, we compared the ED trajectories assessed from signals of the complete set of 120 leads (BSPM) and a reduced lead set of the standard 12-lead ECG (six precordial and three augmented limb leads). To increase the space isotropy of leads, we used a modified Leadset2 with the V2, V3 and V4 leads replaced by EASI leads I and S, and the dorsal Nehb lead D, respectively.

The inversion matrix necessary for calculating surface potentials was obtained by tailoring a model torso to fit the electrode positions, which provided the model torso parameters. Relative volume conductances of the lung, abdominal, and heart tissue at the anatomically expected sites under the torso surface were taken as arbitrary values of 0.5, 1, and 2, respectively. For the initial estimate set of EDs, we assumed that they move along the ED trajectory in the direction of the instantaneous ED orientation.

Besides representing trajectory patterns in the x, y, and z coordinate system with the frontal, transversal, and sagittal planes, we also made representations in the heart's local coordinate system (Figure 2), assuming that each heart follows the mean heart orientation within the thorax, obtained from cardiac MRI studies [8]. Due to the unknown position of the heart, we assumed that during depolarization, the trajectory center coincides with the ventricular center.

2.5. Comparison of the trajectory patterns

To assess differences in the trajectory pattern of the QRS interval between different lead sets, we compared the corresponding positions, sizes and spatial trajectory orientations. Differences in position were evaluated by the mutual offset $\Delta\mathbf{r}_{tr}$ of the trajectory center (mean location of all moving EDs in the QRS interval). Differences in the trajectory size were obtained by comparing the mutual trajectory length l expressing it as the length ratio l_1/l_2 to the BSPM set. Differences in the

trajectory orientation were obtained by fitting a line to each trajectory with direction cosines, $\boldsymbol{\alpha}_{lin1}$ and $\boldsymbol{\alpha}_{lin2}$, respectively, to determine deviation angle $\Delta\alpha_{lin}$.

For testing local congruency in the trajectory direction between different lead sets we calculated mean deviation angle $<\Delta\alpha_{Tr}>$ over the QRS interval between corresponding instantaneous trajectory directions, $d\mathbf{r}_k/|\mathbf{dr}_k|$, utilizing the dot product of direction cosines, where $d\mathbf{r}_k$ is the spatial derivative of trajectory. Similarly, for testing dipole orientation congruency, we determined mean deviation angles $<\Delta\alpha_D>$ of the instantaneous dipole orientations, $\mathbf{D}_k/|\mathbf{D}_k|$, between the two lead sets. All angles were expressed in degrees [º].

For a perfect congruence of the trajectories, angles $\Delta\alpha_{lin}$, $<\Delta\alpha_{Tr}>$, and $<\Delta\alpha_D>$ should approach 0, $\Delta\mathbf{r}_{tr}$ zero, and l_1/l_2 1.

To test a hypothesis that the ED trajectory direction is aligned with the ED orientation, we determined the mean angle $<\Delta\alpha_{DTr}>$ calculated from the instantaneous values of $\Delta\alpha_{DTr} = d\mathbf{r}_k/|\mathbf{dr}_k| \cdot \mathbf{D}_k/|\mathbf{D}_k|$ (Figure 2). To confirm the hypothesis, $<\Delta\alpha_{DTr}>$ should approach zero.

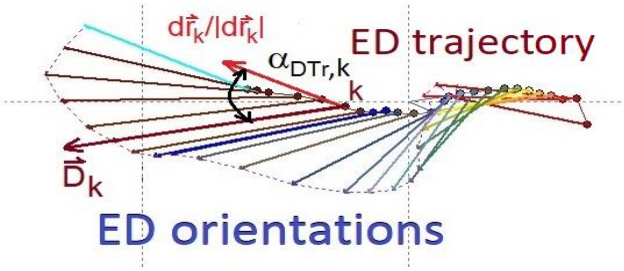

Figure 2. Definition of the mean angle $<\Delta\alpha_{DTr}>$ to test the aligned ED trajectories and orientations hypothesis.

3. Results

In all lead sets, the ED trajectory directions were consistent with the annotated pacing sites, with EDs moving from the pacing site in directions towards the ventricular center (Figure 3).

In LeadSet1, the trajectory offset $|\Delta\mathbf{r}_{tr}|$ was 1.7±1.0 cm (mean±SD) with x, y and z components equal to 0.2±0.9 cm, -0.1±1.6 cm, and 0.3±0.9 cm, respectively. The trajectory length ratio l_1/l_2 was 0.91±.0.19 at the BSPM trajectory length of 4.4±1.3 cm. The dipolar deviation angle with a median $<\Delta\alpha_D>$ of 10.5º was significantly smaller than that of the trajectory pattern orientation $\boldsymbol{\alpha}_{lin}$ and trajectory direction $d\mathbf{r}_k/|\mathbf{dr}_k|$ with median values of $\Delta\alpha_{lin}$ = 16.4º and $<\Delta\alpha_{Tr}>$ = 28.2º, respectively (Table I).

In LeadSet2, the trajectory offset $|\Delta\mathbf{r}_{tr}|$ was slightly smaller, 1.3±0.6 cm with x, y and z components 0.3±0.7 cm, -0.2±0.4 cm, and 0.4±0.9 cm, and l_1/l_2 was1.02±0.19. The corresponding dipolar and trajectory distributions were similar to LeadSet1with median $<\Delta\alpha_D>$ of 15.9º, $\Delta\alpha_{lin}$ of 15.3º and $<\Delta\alpha_{Tr}>$ of 23.2º (Table I, Figure 4).

Median values of mean angles $<\Delta\alpha_{DTr}>$ between instantaneous dipolar orientation and trajectory direction in the BSPM set, LeadSet1, and LeadSet2 were 22.8º, 31.2º, and 25.8 º, respectively.

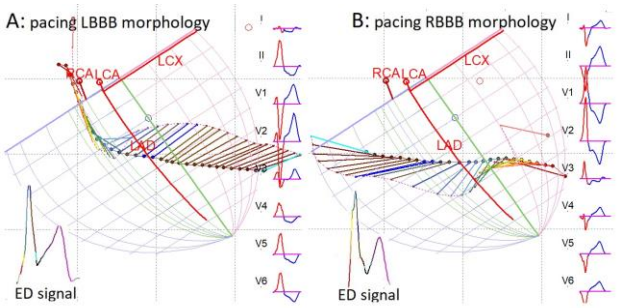

Figure 3. ED trajectories with ED orientation from the 12-lead ECG in the four-chamber view with two ventricles. A: pacing with LBBB morphology, B: pacing with RBBB morphology. Right: the standard 12 lead ECG. The ED amplitude signal provides color coding of EDs. The ventricles with the coronary arteries, LAD, LCX, and RCA, are positioned so that the LeadSet1 trajectory center coincides with the ventricular center.

Table I. Median and percentile values obtained by comparing trajectory pattern properties of 17 recordings of the reduced and BSPM lead sets.

LeadSet1 and BSPM set comparison						
	$\lvert\Delta\mathbf{r}_{tr}\rvert$ [cm]	l_1/l_2 [rel]	$<\Delta\alpha_D>$ [º]	$\Delta\alpha_{lin}$ [º]	$<\Delta\alpha_{Tr}>$ [º]	$<\Delta\alpha_{DTr}>$ [º]
median	1.53	0.89	10.5	16.4	28.2	30.3
5th %	0.44	0.66	74	4.5	19.2	21.6
95th %	3.24	1.28	23.0	40.0	39.9	43.5
LeadSet2 and BSPM set comparison						
median	1.30	0.96	15.9	15.3	23.2	25.7
5th %	0.63	0.72	7.9	6.0	14.6	21.4
95th %	2.24	1.47	25.1	39.2	32.1	33.6

$|\Delta\mathbf{r}_{tr}|$, the absolute difference in the trajectory center positions; l_1/l_2, relative trajectory length ratio; $<\Delta\alpha_D>$, mean angle between mutual dipole orientations; $\Delta\alpha_{lin}$, the angle between the trajectory pattern orientation; $<\Delta\alpha_{Tr}>$, mean angle between mutual instantaneous trajectory directions; $<\Delta\alpha_{DTr}>$, mean angle between instantaneous dipole orientations and trajectory directions;

4. Discussion and conclusions

We found a considerable resemblance in the trajectory shape and size between both reduced lead sets, LeadSet1 or LeadSet2, and the BSPM set, and both lead sets provided similar results. The trajectory pattern was displaced by roughly 1.5 cm, it was rotated by 15º and slightly shorter than in BSPM, as estimated from median values of of $|\Delta\mathbf{r}_{tr}|$, $\Delta\alpha_{lin}$, and l_1/l_2, respectively.

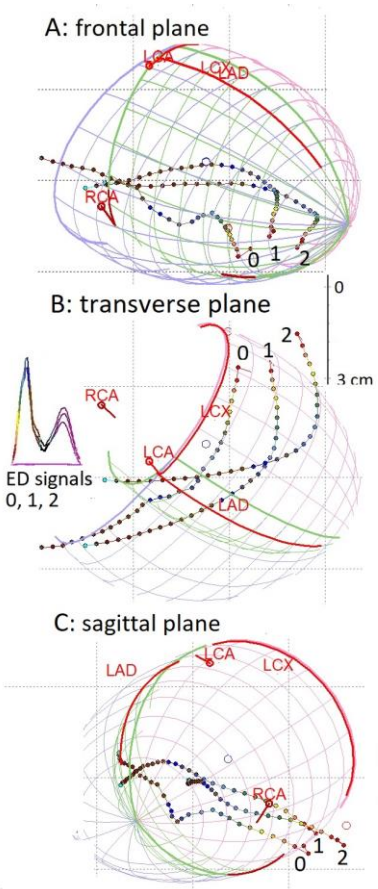

Figure 4. Comparison of ED trajectories from the recording with the median $<\Delta\alpha_{Tr}>$ value obtained with different lead sets. A: The frontal plane, B: the transverse plane, and C: the sagittal plane. ED Trajectories from BSPM, LeadSet1, and LeadSet2 are denoted by 0, 1, and 2, respectively. The ED amplitude signal provides color coding of EDs. The ventricles with the coronary arteries, LAD, LCX, and RCA, are positioned so that the BSPM trajectory center coincides with the ventricular center.

Mean angle deviations in the trajectory direction were nearly twice bigger with median $<\Delta\alpha_{Tr}>$ between 25 and 30º. They were connected mainly by local deviations of the ED trajectory form the straight line with α_{lin} due to imperfect regularization of other variables that ED position, $\mathbf{r}_k$. The ED orientation distribution with median $<\Delta\alpha_D>$ between 10º and 16º performed much better and was more stable due to $\mathbf{r}_k$ variation during optimization.

Many factors might be responsible for less accurate determination of ED trajectory patterns from the reduced lead sets. Besides the precision of the applied BEM, the accuracy of the trajectory pattern determination depends on the quality of the recorded signal, on the presence of multipoles [9], and on the signal information content, which depend on dipolar strength and particularly on the isotropy of ED orientations. The latter is consistent with our findings that the worse congruence was obtained in cases with predominant ED orientations in the cranio-caudal direction, which is covered only by lead II in the standard 12-lead ECG. As the replaced leads in LeadSet2 did not improve the results significantly, the reason for inaccuracy may also lay in the applied BEM, particularly the volume conductance values of the model, which calls for further investigation.

Despite rather considerable trajectory offset and angle deviations of 15º, the trajectory patterns look similar (Figure 4). So, we believe that assessing the ED trajectory with this accuracy may help improve the detection of depolarization abnormalities in the clinical setting.

Similarly, the failure to prove the aligned ED trajectories and orientations hypothesis does not talk against its clinical applicability, at least when used as a reasonable initial estimate of the position of sources.

Further research in ECGs with various pathology is necessary to investigate the possible applicability of this analysis in future ECG diagnostic algorithms.

References

[1] V. Starc, and T.T. Schlegel, “Moving dipole determination from 12-lead ECGs can improve detection of acute myocardial Ischemia,” Computing Cardiol., vol. 47, pp.1-4, 2020.

[2] W. Bystricky, “Identification of strict left bundle branch block using a moving dipole model,” Computing in Cardiol., vol. 45, p.1-4, 2018

[3] P.M. van Dam, "A new anatomical view on the vector cardiogram: The mean temporal-spatial isochrones," J. Electrocardiol., vol. 50, p.732–738, 2017.

[4] T.F. Oostendorp and A. van Oosterom, "Source parameter estimation in inhomogeneous volume conductors of arbitrary shape". IEEE Trans. Biomed. Eng., vol. 36, p.382-391, March 1989.

[5] A.J. Pullan, L.K. Cheng, R. MacLeod, D.H. Brooks, et al., ”The Inverse Problem of Electrocardiography”, In: P.W. Macfarlane et al. (eds.), Comprehensive Electrocardiology, p. 299-344. Springer, London 2010.

[6] J.L. Sapp, F. Dawoud, J.C. Clements, and B.M Horáček, "Inverse solution mapping of epicardial potentials: Quantitative comparison with epicardial contact mapping," Circ. Arrhythm. Electrophysiol., vol. 5, p.1001-9, 2012.

[7] K. Aras, W. Good, J. Tate, R. MacLeod, et al., “Experimental Data and Geometric Analysis Repository-EDGAR“. J Electrocardiol., vol. 48, p. 975–981, 2015.

[8] F. Odille, S. Liu, P. van Dam, and J. Felblinger, “Statistical variations of heart orientation in healthy adults,” Computing Cardiol., vol. 44, pp.1-4, 2017.

[9] V. Starc, “Moving equivalent multipoles derived from the body surface potential map by solving the inverse problem,” Computing Cardiol., vol. 37, p.875-8, 2010.

Address for correspondence:
Vito Starc, MD, PhD
Ljubljana University, Faculty of Medicine
Zaloska 4, SI 1000 Ljubljana, Slovenia
E-mail: vito.starc@mf.uni-lj.si